



# On the Physical Properties of G-Type Main Sequence Stars

Bijan Nikouravan , Misha Nikouravan 

Department of Physics, Islamic Azad University (IAU), Varamin, Pishva Branch, Iran  
Department of Mechanical Engineering, Sharif University of Technology, Kish International Campus, Iran

[nikouravan@gmail.com](mailto:nikouravan@gmail.com)

Received March 2023

Received in revised: April 2023

Published: Jun 2023

## ABSTRACT

This research focuses on the classification and properties of G-Type main sequence stars. It discusses the historical development of star classification systems and their importance in understanding stellar evolution, composition, and galactic structures. The paper also examines the mass-radius and mass-luminosity relationships of stars, highlighting the strong positive correlations between mass and radius, as well as mass and luminosity. The findings suggest that more massive stars tend to be larger and more luminous. However, further analysis is needed to explore the underlying relationships between these variables.

**Keywords:** Steller Classifications, G-Type main sequence stars, New discovered exoplanets.

©2023 The Authors. Published by Fundamental Journals. This is an open-access article under the CC BY-NC  
<https://creativecommons.org/licenses/by-nc/4.0/>

## INTRODUCTION

Stars have fascinated humans for centuries, and their classification has been a subject of keen interest among astronomers. The classification of stars can be done on the basis of a single observable property of the objects, or a combination of properties. The need to classify stars arose from the desire to understand their diverse characteristics and to make sense of the vast number of stars in the universe. Several classification systems have been developed over time to categorize stars based on various parameters, such as their spectral characteristics, luminosity, and evolutionary stage (Jaschek & Jaschek, 1990).

The earliest attempts at star classification can be traced back to the late 19th century when the Harvard Spectral

Classification System was introduced (Jaschek & Jaschek, 1990; Pickering, 1890). This system classified stars based on their spectral types, such as O, B, A, F, G, K, and M. It laid the foundation for subsequent classification systems.

In the early 20th century, the Yerkes Spectral Classification System, introduced around the 1900s, expanded upon the Harvard system (Morgan, Keenan, & Astrophysics, 1973). It added additional spectral types, such as L and T, to accommodate the diversity of stars. Simultaneously, the luminosity class system (early 20th century) emerged, which categorized stars based on their brightness or luminosity. This system classified stars into different classes, ranging from I (Supergiant stars) to V (main sequence stars) (Luminosity class system, 1900s) (Morgan et al., 1973). To better understand the relationship between a star's characteristics and

its evolutionary stage, the Hertzsprung-Russell (HR) Diagram was formulated in the early 20th century (Hertzsprung, 1947). This graphical representation plotted stars' luminosity against their temperature, providing insights into stellar evolution. In the 1940s, the MK Spectral Classification System was introduced, building upon the Harvard system (Jaschek & Jaschek, 1990; Morgan, Keenan, & Kellman, 1943; Morgan et al., 1973). It assigned numerical values to each spectral type, resulting in a more quantifiable classification scheme. Further advancements came with the Extended Yerkes Spectral Classification System in the 1950s, which incorporated additional spectral types and subclasses (Wilson, Childs, & Edith, 1943). These additions allowed for a more comprehensive description of the observed stars. In the 1960s, the Morgan-Johnson-Gottfried (MJG) System was established, which extended the MK system by incorporating not only spectral types but also luminosity, temperature, and chemical composition (Abt & Bidelman, 1969). This comprehensive classification scheme provided astronomers with a detailed understanding of various stellar properties.

The classification of stars serves several purposes. Firstly, it helps astronomers organize and categorize the vast number of stars observed in the universe. By classifying stars based on their spectral characteristics, luminosity, and other parameters, astronomers can easily identify and study different types of stars (Bailer-Jones, 2001). Secondly, star classification allows for the identification of patterns and trends in stellar properties. By grouping stars into different classes and subclasses, astronomers can analyze the relationships between various stellar characteristics and gain insights into stellar evolution, composition, and other important aspects of stellar astrophysics.

Additionally, classifying stars facilitates the study of stellar populations and the understanding of galactic structures. By examining the distribution of different types of stars within galaxies and across the universe, astronomers can gain valuable information about the formation and evolution of galaxies (Brinchmann et al., 2004). Overall, the classification of stars is a fundamental aspect of astronomy that helps us comprehend the diversity and properties of stars in the universe (Percy, 2007). The various classification systems developed over time have provided astronomers with valuable tools for studying and understanding the vast celestial objects that have captured our curiosity and imagination (Burnham, 2013; Jaschek & Jaschek, 1990).

The purpose of this paper is to investigate the relationships between mass, radius, temperature and luminosity of all newly discovered stars. In the following, we will examine the newly discovered stars that are located in the temperature range of 5000-6000 degrees Kelvin and are known as the G-Type main sequence.

We will examine the relations between radius-mass, mass-luminosity, mass-temperature and relation with luminosity for stars and we will deal with their correlation.

According to the data obtained from the exoplanets that are in the G-Type main sequence star group, the importance of these planets is more important due to the possibility of life (Hernández et al., 2013). For this reason, in this article we will try to examine the newly discovered exoplanets that are in this group. Studying the correlation of mass, radius, and temperature for this group of exoplanets is also one of the goals of this article. All the data studied in this article is collected from the NASA Exoplanet Archive (Institute, 2020), which

was recently published in 2023. We will also have an answer to the relationship between more massive, bigger and brighter stars.

## STELLAR PROPERTIES

Stellar properties refer to the characteristics and attributes of stars that astronomer's study and analyze. These properties provide valuable insights into a star's nature, behavior, evolution, and its impact on surrounding objects like planets or other stellar systems. Understanding stellar properties is crucial for various fields of astrophysics, including stellar astronomy, galactic dynamics, cosmology, and exoplanet studies. The Hertzsprung-Russell (H-R) diagram is a scatter plot that correlates two essential stellar parameters, luminosity versus and surface temperature (Inglis, 2015). It provides valuable information about different stages of stellar evolution by revealing patterns such as the main sequence, giants, supergiants, white dwarfs, etc. The Luminosity-Temperature diagram of 809 stars, between 2000-and 10000-degrees Kelvin has been shown in Figure 1.

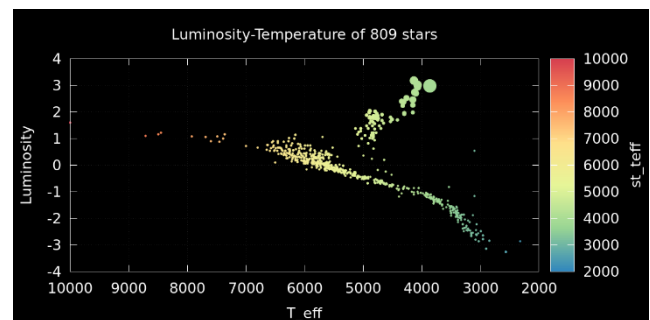


Fig 1: Luminosity-Temperature diagram for 809 Stars.

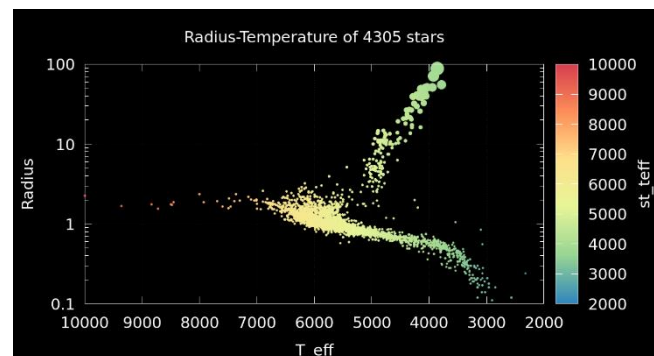


Fig 2: Radius-Temperature of 4305 Stars. The radius is between 0.1 to 100 solar radius and the temperature is from 2000 to 10000 Kelvin.

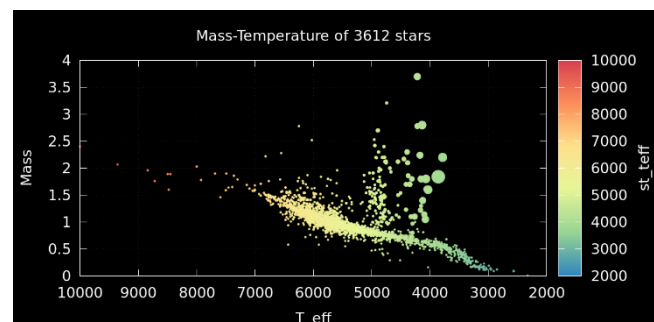


Fig 3: The Mass-Temperature diagram for 3612 Stars.

### MASS-RADIUS RELATIONSHIP (M-R)

According to latest data collection by 2023, there is a general relationship between stars mass and their radius. This relationship is influenced by factors like stellar composition, internal structure (core density/pressure), evolutionary stage, etc., but it provides insights into how stars are structured physically. Figure 4 show a correlation relationship between the radius and mass of 2471 stars. Here the temperature of stars

is selected from 2000 to 7000 kelvins. The Sun position shown with for  $R = 1$  and  $M = 1$  (Figure 4). Here the x-axis as stellar radius, is between 0.11 and 1.5 in solar radius. The minimum value of 0.11 and the maximum value of 1.5 indicate the range of stellar radii observed in the data. The median value of 0.92 suggests that half of the stars in the dataset have a radius smaller than 0.92, while the other half have a radius larger than 0.92. The mean value of 0.920271 represents the average radius of the stars in the dataset.

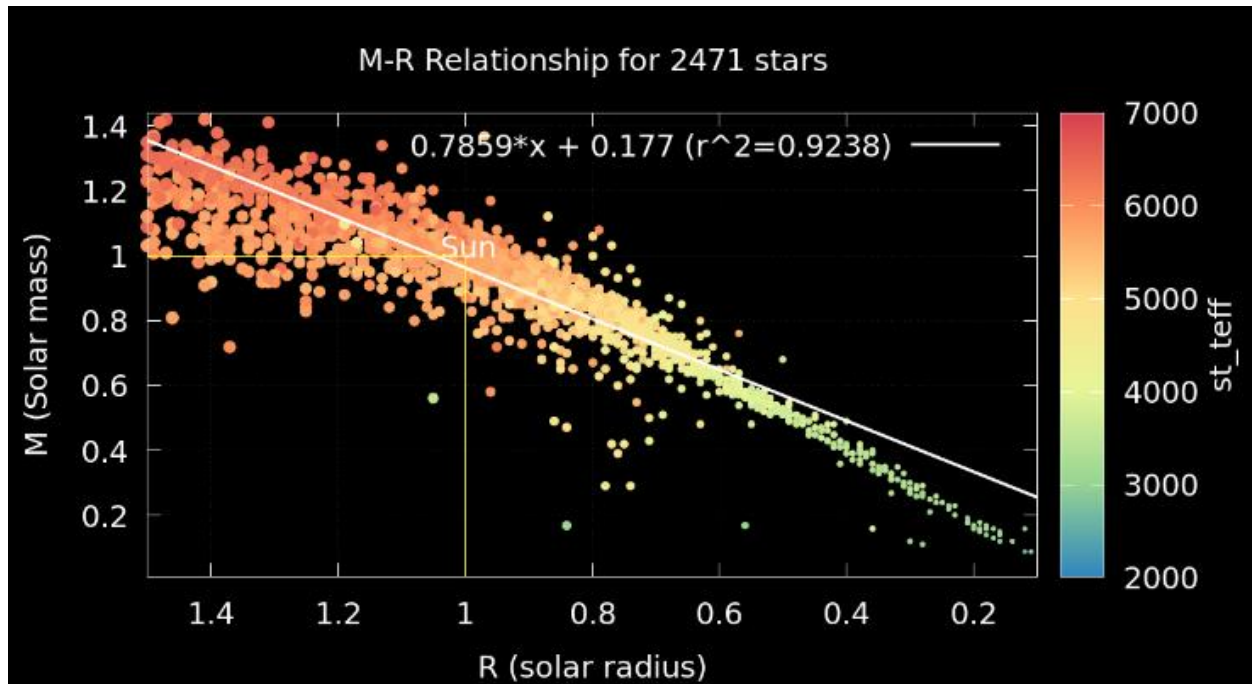


Fig 4: M-R for 2471 stars. The position of Sun shown in for  $R_{sun} = 1$  and  $M_{sun} = 1$ .

For the stellar mass we find a minimum value of 0.01 and a maximum value of 1.44 and it is indicated the range of stellar masses observed. The median value of 0.94 suggests that half of the stars have a mass smaller than 0.94, while the other half have a mass larger than 0.94. The mean value of 0.900 represents the average mass of the stars in the dataset.

But for stellar effective temperature. This variable indicates that the minimum value of 2320 and the maximum value of 6594 are in the range of temperatures observed. The median value of 5566 suggests that half of the stars have a temperature below 5566, while the other half have a temperature above 5566.

The 25th percentile is 0.765, the median is 0.92, and the 75th percentile is 1.09 and the mean (average) value for this variable is equal to 0.920271. Moreover, in the y-axis that is presented for mass of stars, the minimum and maximum values are 0.01 and 1.44 respectively. The 25th percentile is 0.8, the median is 0.94, and the 75th percentile is 1.04 and the mean value is also 0.9.

The size and color of these stars are indicated in the radius and temperature of stars. The temperature for stars is from 2000 to 7000 kelvins. The 25th percentile is 5006.5, the median is 5566, and the 75th percentile is about 5865.5.

From our statistical calculation, it appears that between the mass and temperature of stars, we have a much stronger positive correlation with value of  $R^2 = 0.941287$ . This value

indicates a strong positive correlation and it means that as the mass of the star increases, then the star's temperature also tends to increase, and vice versa  $M \propto T$ .

And between the star radius and surface temperature (stellar effective temperature) of stars, we have also a strong, but a slightly weaker positive correlation than the M-T with value of  $R^2 = 0.898338$ . This correlation coefficient suggests that as the radius of stars increases, the stars surface temperature also tends to increase, and vice versa. However, this correlation is slightly weaker compared to the correlation between the radius and mass of stars  $R \propto T$ .

It is exciting to observe that the radius and mass of stars also share a strong positive correlation with value of 0.923792. This indicates that as stellar radius increases, stellar mass tends to increase as well. Similarly, as star radius decreases, star masses tend to decrease.

In other words, an increase in mass is equivalent to an increase in radius and vice versa, that is, the relationship between mass and radius in stars is a direct relationship.  $M \propto R$ . Overall, these correlations suggest that there are relationships between the variables  $R$ ,  $M$ , and  $T$ . Changes in  $R$  and  $M$  tend to occur together, while changes in  $M$  and  $T$  also tend to occur together. However, it's important to note that with these correlations we need further analysis to understand the underlying relationships between these variables.

## MASS-LUMINOSITY RELATIONSHIP (M-L)

The Mass-Luminosity Relationship is a fascinating topic when it comes to stars in the main sequence. It describes the relationship between a star's mass and its luminosity, which is the total amount of energy it emits per unit time. In general, the Mass-Luminosity Relationship tells us that more massive stars tend to be more luminous than less massive ones. This means that as a star's mass increases, its luminosity also increases. However, the relationship is not purely linear. It follows a power law, meaning that the increase in luminosity is not proportional to the increase in mass. Specifically, the Mass-Luminosity Relationship is often expressed using the equation.

$$L \propto M^\alpha$$

where  $L$  represents the star's luminosity,  $M$  represents its mass, and  $\alpha$  is the exponent that determines the power law relationship. Interestingly, the exponent  $\alpha$  is typically found to be greater than 1, which means that the increase in luminosity is more than proportional to the increase in mass. This is because more massive stars have higher core temperatures and pressures, which leads to more efficient energy production through nuclear fusion. The value of  $\alpha$  in the Mass-Luminosity Relationship for stars in the main sequence has been a subject of ongoing research and study.

Over the years, different studies have estimated varying values for  $\alpha$  based on observations and theoretical models. Traditionally, a commonly accepted value for  $\alpha$  was around 3.5. However, more recent research has suggested that the value might be closer to 4 or even slightly higher. These new results are based on improved observational data, advances in stellar models, and a better understanding of the physics involved in stellar evolution. Here, the relationship between luminosity and mass shows a strong and good linear relationship, but we do not rule out the non-linear relationship mentioned above.

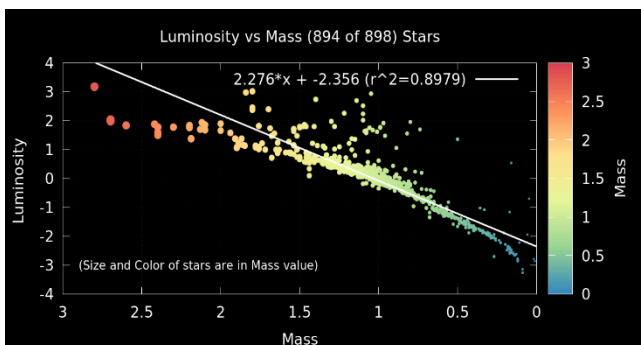


**Fig 5:** Luminosity vs Mass (894 of 898) Stars. (Size and Color of stars are in Mass value)

Here the correlation coefficient between mass and luminosity is 0.897892. This indicates a strong positive correlation between mass and luminosity. As mass increases, luminosity tends to increase as well. It's important to note that the Mass-Luminosity Relationship is an average relationship and there can be some variations among different stars due to other factors such as age, chemical composition, and stellar evolution.

## M-L RELATIONSHIP FOR KNOWN L

According to new findings, 3953 stars have been identified by 2023. Of these, the luminosity of only 933 stars has been computed, and the luminosity of 2918 stars has not been calculated yet. Considering that the luminosity is known and also the mass of the stars is known, the graph between mass and luminosity is drawn as below (Fig 3). The correlation coefficient of this graph is around 0.8966. This correlation shows evidence of a strong relationship between the mass of the star and its luminosity. But we note that this correlation is for 933 stars out of all (3953) detected stars. This is before our calculation for luminosity. In this case we had 933 stars with  $L$  known.

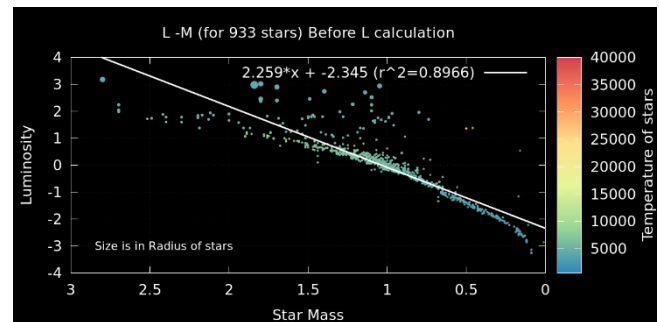


**Fig 6:** Out of 3953 stars only 933 stars luminosity was known. The correlation of L-M for 933 stars is  $R^2 = 0.8966$ .

The Figure 6 shows all known and available data for 933 stars to draw luminosity-mass relationship out of 3953 stars. The minimum and maximum mass for stars is  $0.01 \leq M_s \leq 2.8$  of solar mass with luminosity between -3.257 to 3.17 in solar luminosity. The size of selected stars is in the radius between 0.01 to 88.47 of solar radius with the mean value of 1.52213. The lowest and highest temperature observed among these stars is between 575 to 40000 kelvins.

The correlation coefficient between luminosity and mass of stars shows  $R^2 = 0.8966$ . These properties in Fig 6 is exactly before our calculation for luminosity of stars. It should be mentioned that all these values are according to the values obtained directly from the NASA website and a large number of values will be calculated for luminosities in the next section.

## M-L RELATIONSHIP FOR UNKNOWN L (AFTER OUR L CALCULATION)

As mentioned in the previous section, we selected the properties of 3951 stars from the NASA data system. From this amount of data, only the luminosity characteristics of 933 stars has been known, and the luminosity of 2918 stars is still unknown but is calculatable.

The purpose of this section is to estimate the luminosity of 2918 stars. Certainly, by calculating these number of unknown values we can get more information and understanding the stars conditions which is shown in Fig 7.

After calculation of luminosity for 2918 stars, the statistical work founded shows that the minimum and maximum masses of stars is  $0.01 \leq M_s \leq 2.8 M_\odot$  of solar mass (same as Fig 6) and the luminosity of stars are from -3.252 to 3.192  $L_\odot$  in solar luminosity.

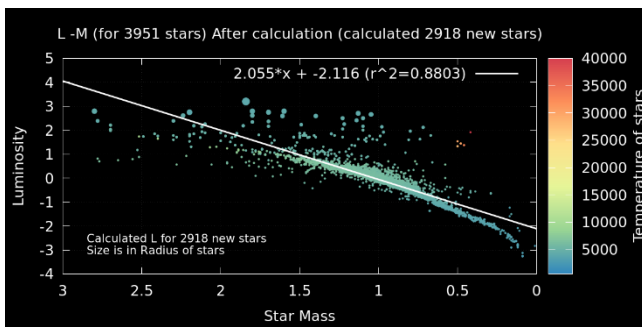


**Fig 7:** Luminosity – Mass relationship. The total stars are about 3951 and number of calculated unknown luminosities is 2918 with  $R^2 = 0.8803$ .

The size of stars also shown in Fig 7 is in terms of solar radius and between  $0.11$  to  $88.47 R_{\odot}$  with the mean value of  $1.52213$ . The temperature of stars selected between  $2000$  to  $40000$  kelvins. The information shows a strong positive correlation between luminosity and star's mass in range of  $R^2 = 0.8803$  (Fig 7). This suggests that as stellar masses increase or decrease relative to solar masses, their calculated luminosities also tend to increase or decrease proportionally. As well there exists a moderate positive correlation between the radii and mass of stars with a coefficient of about  $0.402165$ , indicating that as stellar masses increase or decrease relative to solar masses, their radii tend to increase or decrease, albeit with less strength compared to the correlation between mass and luminosity. Moreover, star mass and temperature show a weak positive correlation with a coefficient of approximately  $0.324783$  and this implies that there is some tendency for stellar masses relative to solar masses to influence effective temperatures, although the relationship is not particularly strong.

A moderate positive correlation between luminosity and temperature of stars correspondingly is approximately about  $0.478248$ . As calculated luminosities increase or decrease, relative to solar luminosities, corresponding changes in effective temperature are observed. Likewise, a moderate positive correlation between the luminosity and the radius of the stars with a coefficient of about  $0.505441$  has been observed. This shows that as the calculated luminosities increase or decrease relative to the solar luminosities, the stellar radii tend to increase or decrease accordingly. It is worth mentioning that all data indicated in Fig 7 is exactly after calculation of 2918 unknown luminosity out of 3951 stars.

### M-L RELATIONSHIP FOR G-TYPE STARS

According to the experimental data and the observations made for the stars belonging to the G-group, these group of stars have the properties and characteristics in mass, temperature, luminosity and radius are as well as other stars, but the effective temperature of G-type stars typically ranges from around  $5,000$  to  $6,000$  Kelvin. This range represents the average temperatures for G-dwarf stars. Similarly, the G-type main-sequence stars have masses that range from approximately  $0.8$  to  $1.2$  times the mass of our Sun ( $M_{\odot}$ ). The luminosity of these group of stars is generally between  $0.6$  to  $1.5$  times of the solar luminosity ( $L_{\odot}$ ) which is corresponds to an energy output ranging from approximately  $60\%$  to  $150\%$  compared to our Sun. Moreover, average radius of these group of stars falls within a range of about  $0.9$  to  $1.5$  times the radius of our Sun ( $R_{\odot}$ ).

The habitable zone around these stars refers to the region where conditions may be suitable for liquid water and potentially life as we know it exists on planetary surfaces and it is in inner and outer edge. For the inner edge or boundary is determined by how close a planet can orbit without its surface water evaporating due to intense stellar radiation and for the outer edge or boundary depends on factors such as atmospheric composition, greenhouse effects, cloud cover, etc., which affect temperature stability and prevent water from freezing entirely. It's important to note that these values represent general trends and averages observed in scientific studies based on observations and theoretical models of various known G-type main-sequence stars in our galaxy. However, individual stars within this spectral type may exhibit variations in their properties due to factors like metallicity (abundance of elements heavier than hydrogen and helium), age, rotation rate, presence of companions or planets influencing their evolution, and other stellar characteristics.

Since our main goal in this paper is to consider place G group stars at their predefined temperature, we will therefore examine the newly discovered stars of this group. Consequently, we follow the defined temperature of this group of stars by Hertzsprung and Russell diagram which is between  $5000$ - and  $6000$ -degrees Kelvin. Now, by finding new stars discovered until today (2023) in the same temperature range, it gives us a little different definition in mass, radius and luminosity. By considering this temperature range, it can be seen that the changes in mass, radius and luminosity of this group of stars lead us to other new characteristics of this group (G-Type). According to data collection from NASA Exoplanets Archive, we counted 2121 stars in the range of  $5000$ - $6000$  kelvin. (Fig 8).

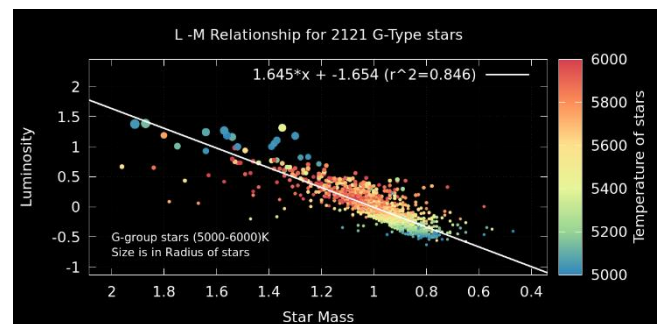


**Fig 8:** L-M Relationship for 2121 computed G-type stars

According to the previous section for computing 2918 unknown luminosities of stars, we found that 2121 stars belong into the G-Type main sequence stars. As already mentioned, the temperature of these group of stars are between  $5000$  to  $6000$  Kelvin (Fig 8). Accordingly, the minimum and maximum mass of stars is  $0.47 \leq M_s \leq 1.96 M_{\odot}$  of solar mass. As for the luminosity, we have the values between  $-0.635$  to  $1.386 L_{\odot}$  in solar luminosity. The size of these stars in terms of solar radius is in the range of  $0.57$ - $6.43 R_{\odot}$  of solar radius, with the mean value of  $1.07185$ . Consequently, the correlation index between mass and luminosity is  $R^2 = 0.846$ .

All properties in figure 5 is exactly according to our luminosity calculations between  $5000$  to  $6000$  Kelvin for G-Type of main sequence stars. The minimum mass value in the dataset is  $0.47$  times the mass of our Sun. From the statistical values, approximately  $25\%$  of stars have a mass less than or equal to  $0.89$  times the solar mass. The maximum mass value in the

dataset is 1.96 times the solar mass and with the average (mean) mass value of 0.978 times that of our Sun. For the luminosity, the minimum value in the dataset is about -0.635, which should be interpreted relative to other data points rather than absolute units. Similar to above, these values represent positions within the distribution but not absolute luminosities. On average, the stars in this dataset have a slightly negative mean luminosity (-0.046), indicating they are less bright compared to our Sun on average. The radius of stars in these group values (Minimum through Maximum) represent ranges and extremes within which radii vary among G-Type Main-Sequence stars in this dataset. On average, G-dwarf stars have a mean radius around 1.072 times that of our Sun with a standard deviation of roughly  $\pm 0.474$ . The correlation matrix from the graph provides information about how strongly two variables are linearly related. The relationship between star mass and star luminosity (L-M) show a correlation coefficient of approximately  $R^2 = 0.846$ , that indicating a strong positive linear relationship between mass and luminosity. The correlation between temperature and luminosity (T-L) is in the

range of  $R^2 = 0.6158$  and a correlation between luminosity and radius (L-R) of stars is equal to  $R^2 = 0.8297$ .

We have kept in mind that these interpretations are based solely on statistical analysis without considering any physical context or specific astrophysical theories related to star formation or evolution. More research is also needed to examine and investigate the physical properties of the studied stars.

### EXOPLANETS SEMI-MAJOR AXIS VS PLANETS ORBITAL PERIOD

In G-Type main sequence stars, we are also interested in investigating the new exoplanets in this group. By accessing the latest data obtained from the NASA website, 248 new exoplanets were found in this group. But we are able to consider the relationship between semi-major axis vs planets orbital period of 103 planets (see Fig 9). All the exoplanets found here are belong to stars with temperature range of 5000 (or roughly 5200) to 6000 K.

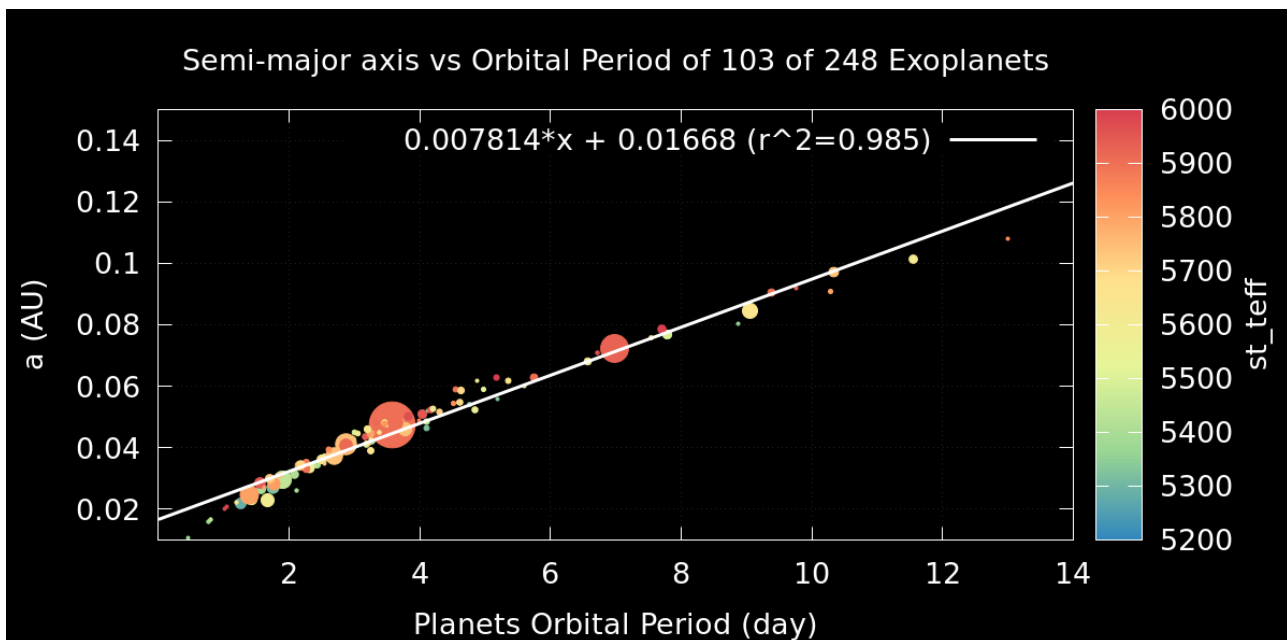


Fig 9: Planets Semi-major axis (AU) vs Planets Orbital Period (day). (103 Exoplanets out of 248) size is in mass of planets  $R^2=0.985$

In fact, all of these stars are quite special, and the planets orbiting them have some exciting characteristics, such as habitable zone conditions that may be suitable for liquid water to exist on planetary surfaces, and therefore planets located within this region have the potential to support life as we know it. The periods of orbits for these planets can range from days to years and some planets in this group have nearly circular orbits or low eccentricity, while others may possess more elongated elliptical paths. Some planets have nearly circular orbits or low eccentricity, while others planets may possess more elongated elliptical paths. There is an increased likelihood of finding rocky exoplanets in close-in orbits around G-Dwarfs due to their size and mass distribution compared to larger gas giants. Moreover, the similarity in size, temperature, and luminosity of these stars relative to our Sun, offers favorable conditions for hosting potentially Earth-like worlds capable of supporting liquid water and potentially even

life. Today researchers study exoplanet atmospheres through spectroscopic observations aiming at detecting chemical signatures such as water vapor, carbon dioxide, methane, etc., which provide insights into planetary composition and potential habitability. It's important to note that discovering and exploring exoplanets around G-Type main sequence stars is an ongoing scientific endeavor. In the Fig 9, the x-axis represents the orbital period of the planets, measured in days, and the y-axis also represents the semi-major axis of the planets' orbits, measured in astronomical units (AU). The size of planets here are in the mass of the planets and the color represents the effective temperature of the stars that the planets orbit around. The smallest value observed in each respective variable indicates the minimum orbital period about 0.446569 days, and with semi-major axis of 0.0106 in AU. The minimum effective temperature is about 5280 K.

**Table 1:** List of exoplanets that are in G-Type main sequence stars with computed semi-major axis.

pl name	pl orbper	pl orbsmax	a(cal)	pl rade	st teff	st rad	st mass	st metratio
TOI-2260 b	0.3525	0.0097	0.0097	1.62	5534	0.94	0.99	[Fe/H]
TOI-561 b	0.4466	0.0106	0.0107	1.425	5372	0.84	0.81	[Fe/H]
LTT 9779 b	0.7921	0.01679	0.0154	4.72	5443	0.95	0.77	[Fe/H]
TOI-849 b	0.7655	0.01598	0.0160	3.444	5373.8	0.92	0.93	[Fe/H]
TOI-1416 b	1.0698	0.019	0.0190	1.62	4884	0.79	0.8	[Fe/H]
HD 213885 b	1.0080	0.02012	0.0201	1.745	5978	1.1	1.07	[Fe/H]
TOI-1860 b	1.0662	0.0204	0.0204	1.31	5752	0.94	0.99	[Fe/H]
TOI-2196 b	1.1947	0.02234	0.0223	3.51	5634	1.04	1.03	[Fe/H]
WASP-46 b	1.4304	0.02335	0.0234	13.159	5600	0.86	0.83	[Fe/H]
WASP-135 b	1.4014	0.0243	0.0244	14.572	5675	0.96	0.98	[Fe/H]
CoRoT-1 b	1.5090	-	0.0253	16.7	5950	1.11	0.95	[M/H]
HATS-15 b	1.7475	0.02712	0.0271	12.386	5311	0.92	0.87	[Fe/H]
HD 137496 b	1.6212	0.02732	0.0274	1.31	5799	1.59	1.04	[Fe/H]
WASP-164 b	1.7771	0.02818	0.0282	12.644	5806	0.93	0.95	[Fe/H]
K2-100 b	1.6739	0.0301	0.0289	3.88	5945	1.24	1.15	[Fe/H]
CoRoT-18 b	1.9001	0.0295	0.0295	14.68	5440	1	0.95	[Fe/H]
KELT-14 b	1.7101	0.03005	0.0301	19.537	5720	1.52	1.24	[Fe/H]
Kepler-41 b	1.8556	0.03101	0.0310	14.46	5750	1.29	1.15	[Fe/H]
TOI-157 b	2.0845	0.03138	0.0314	14.415	5404	1.17	0.95	[Fe/H]
TOI-132 b	2.1097	0.026	0.0319	3.42	5397	0.9	0.97	[Fe/H]
WASP-65 b	2.3114	0.0334	0.0334	12.464	5600	1.01	0.93	[Fe/H]
HD 24085 b	2.0455	0.034	0.0337	-	6034	-	1.22	-
HD 158259 b	2.1780	-	0.0338	-	-	1.21	1.08	-
HATS-23 b	2.1605	0.03397	0.0340	20.849	5780	1.2	1.12	[Fe/H]
WASP-133 b	2.1764	0.0345	0.0346	13.563	5700	1.44	1.16	[Fe/H]
WASP-44 b	2.4238	0.03453	0.0346	12.33	5420	0.91	0.94	[Fe/H]
TOI-169 b	2.2554	0.03524	0.0353	12.173	5880	1.29	1.15	[Fe/H]
Kepler-423 b	2.6843	0.03585	0.0358	13.361	5560	0.95	0.85	[M/H]
HATS-4 b	2.5167	0.0362	0.0362	11.433	5403	0.93	1	[Fe/H]
WASP-119 b	2.4998	0.0363	0.0363	15.693	5650	1.2	1.02	[Fe/H]
HD 110113 b	2.5410	0.035	0.0365	2.05	5732	0.97	1	[Fe/H]
TOI-1288 b	2.6998	-	0.0365	5.24	5225	1.01	0.89	[Fe/H]
HATS-54 b	2.5442	0.037	0.0371	11.377	5621	1.23	1.05	[Fe/H]
HATS-16 b	2.6865	0.03744	0.0375	14.572	5738	1.24	0.97	[Fe/H]
HD 307842 b	2.7970	0.038	0.0377	1.93	5558	0.91	0.91	[Fe/H]
Qatar-3 b	2.5079	0.03783	0.0379	12.285	6007	1.27	1.15	[Fe/H]
HAT-P-65 b	2.6055	0.03951	0.0395	21.185	5835	1.86	1.21	[Fe/H]
K2-60 b	3.0027	0.045	0.0403	7.656	5500	1.12	0.97	[Fe/H]
WASP-192 b	2.8787	0.0408	0.0408	13.787	5910	1.32	1.09	[Fe/H]
HD 39855 b	3.2498	0.041	0.0410	-	5576	-	0.87	-
NGTS-18 b	3.0513	0.0448	0.0412	13.563	5610	1.39	1	[Fe/H]
Qatar-5 b	2.8792	0.04127	0.0413	12.408	5747	1.08	1.13	[Fe/H]
HATS-28 b	3.1811	0.04131	0.0413	13.384	5498	0.92	0.93	[Fe/H]
Kepler-426 b	3.2175	0.0414	0.0414	12.22	5725	0.92	0.91	[Fe/H]
TOI-908 b	3.1838	0.041657	0.0417	3.186	5626	1.03	0.95	[Fe/H]
NGTS-15 b	3.2762	0.0441	0.0430	12.33	5600	0.95	0.99	[Fe/H]
NGTS-17 b	3.2425	0.0391	0.0432	13.899	5650	1.34	1.02	[Fe/H]
HAT-P-28 b	3.2572	0.0434	0.0433	13.585	5680	1.1	1.02	[Fe/H]
HAT-P-66 b	2.9721	0.04363	0.0436	17.822	6002	1.88	1.25	[Fe/H]
XO-7 b	2.8641	0.04421	0.0443	15.39	6250	1.48	1.41	[Fe/H]
HD 134060 b	3.2696	0.0444	0.0444	-	5966	-	1.09	[Fe/H]
Kepler-44 b	3.2467	0.0446	0.0446	12.22	5800	1.35	1.12	[Fe/H]
Kepler-77 b	3.5788	0.04501	0.0450	10.761	5520	0.99	0.95	[M/H]
K2-238 b	3.2047	0.046	0.0451	14.572	5630	1.59	1.19	[Fe/H]
WASP-182 b	3.3770	0.0451	0.0452	9.528	5638	1.34	1.08	[Fe/H]
WASP-96 b	3.4253	0.0453	0.0454	13.45	5540	1.05	1.06	[Fe/H]
HD 158259 c	3.4320	-	0.0457	-	-	1.21	1.08	-
WASP-183 b	4.1118	0.04632	0.0463	16.477	5313	0.87	0.78	[Fe/H]

CoRoT-27 b	3.5753	0.0476	0.0465	11.287	5900	1.08	1.05	[M/H]
EPIC 249893012 b	3.5951	0.047	0.0467	1.95	5430	1.71	1.05	[Fe/H]
Qatar-8 b	3.7150	0.0474	0.0474	14.404	5738	1.31	1.03	[Fe/H]
Kepler-101 b	3.4877	0.0474	0.0474	5.77	5667	1.56	1.17	[Fe/H]
CoRoT-17 b	3.7681	0.0461	0.0480	11.43	5740	1.59	1.04	[Fe/H]
WASP-153 b	3.3326	0.048	0.0482	17.374	5914	1.73	1.34	[Fe/H]
WASP-165 b	3.4655	0.04823	0.0483	14.123	5599	1.75	1.25	[Fe/H]
CoRoT-23 b	3.6313	0.048	0.0483	11.77	5900	1.61	1.14	[Fe/H]
K2-30 b	4.0985	0.04839	0.0484	11.646	5425	0.84	0.9	[Fe/H]
NGTS-24 b	3.4679	0.0479	0.0485	13.608	5820	1.64	1.26	[Fe/H]
TOI-1062 b	4.1130	0.052	0.0492	2.265	5328	0.84	0.94	[Fe/H]
HD 86226 c	3.9844	0.049	0.0495	2.16	5863	1.05	1.02	[Fe/H]
61 Vir b	4.2150	0.050201	0.0500	-	5577	0.96	0.94	[Fe/H]
WASP-171 b	3.8186	0.0504	0.0504	10.985	5965	1.64	1.17	[Fe/H]
CoRoT-13 b	4.0352	0.051	0.0511	9.92	5945	1.01	1.09	[Fe/H]
K2-37 b	4.4412	0.0511	0.0511	1.61	5413	0.85	0.9	[Fe/H]
HATS-25 b	4.2986	0.05163	0.0516	14.123	5715	1.11	0.99	[Fe/H]
KELT-10 b	4.1663	0.0525	0.0525	15.681	5948	1.21	1.11	[Fe/H]
CoRoT-26 b	4.2047	0.0526	0.0525	14.12	5590	1.79	1.09	[Fe/H]
HD 149143 b	4.0718	0.053	0.0531	-	5856	1.44	1.2	[Fe/H]
WASP-181 b	4.5195	0.05427	0.0542	13.271	5839	0.96	1.04	[Fe/H]
HATS-5 b	4.7634	0.0542	0.0543	10.223	5304	0.87	0.94	[Fe/H]
HATS-29 b	4.6059	0.05475	0.0547	14.022	5670	1.07	1.03	[Fe/H]
WASP-147 b	4.6027	0.0549	0.0549	12.498	5702	1.43	1.04	[Fe/H]
TOI-733 b	4.8848	0.0618	0.0556	1.992	5585	0.95	0.96	[Fe/H]
NGTS-16 b	4.8453	0.0523	0.0561	14.572	5550	1.21	1	[Fe/H]
HD 213885 c	4.7850	0.056798	0.0569	-	5978	1.1	1.07	[Fe/H]
NGC 2682 YBP 1514 b	5.1180	-	0.0574	-	5725	-	0.96	
CoRoT-31 b	4.6294	0.0586	0.0586	16.365	5700	2.15	1.25	[Fe/H]
WASP-113 b	4.5422	0.05885	0.0589	15.793	5890	1.61	1.32	[Fe/H]
CoRoT-28 b	5.2085	0.0603	0.0590	10.705	5150	1.78	1.01	[Fe/H]
WASP-83 b	4.9713	0.059	0.0591	11.657	5510	1.05	1.11	[Fe/H]
TOI-763 b	5.6057	0.06	0.0601	2.28	5450	0.9	0.92	[Fe/H]
HD 158259 d	5.1981	-	0.0603	-	-	1.21	1.08	-
WASP-131 b	5.3220	0.0607	0.0609	13.675	6030	1.53	1.06	[Fe/H]
CoRoT-16 b	5.3523	0.0618	0.0618	13.11	5650	1.19	1.1	[M/H]
WASP-184 b	5.1817	0.0627	0.0628	14.908	6000	1.65	1.23	[Fe/H]
HD 1461 b	5.7715	0.0634	0.0634	-	5765	-	1.02	[Fe/H]
HD 45184 b	5.8854	0.0644	0.0645	-	5869	-	1.03	[Fe/H]
K2-37 c	6.4290	0.0654	0.0654	2.75	5413	0.85	0.9	[Fe/H]
K2-140 b	6.5692	0.068	0.0677	13.563	5585	1.06	0.96	[Fe/H]
Kepler-101 c	6.0298	0.0684	0.0683	1.25	5667	1.56	1.17	[Fe/H]
HIP 14810 b	6.6739	0.0696	0.0696	-	5544	1.07	1.01	[Fe/H]
HD 110113 c	6.7440	0.068	0.0699	-	5732	0.97	1	[Fe/H]
CoRoTID 223977153 b	6.7184	0.071	0.0715	6.389	5970	0.79	1.08	[Fe/H]
NGC 2682 YBP 1194 b	6.9590	-	0.0716	-	5780	-	1.01	-
TOI-559 b	6.9839	0.0723	0.0722	12.229	5925	1.23	1.03	[Fe/H]
HD 93385 b	7.3426	0.0756	0.0749	-	5977	-	1.04	[Fe/H]
NGTS-12 b	7.5328	0.0757	0.0757	11.747	5690	1.59	1.02	[Fe/H]
HD 96700 b	8.1245	0.0777	0.0761	-	5845	-	0.89	[Fe/H]
TOI-1062 c	7.9720	0.08	0.0765	-	5328	0.84	0.94	[Fe/H]
Kepler-447 b	7.7943	0.0769	0.0770	18.49	5493	1.05	1	[Fe/H]
HD 191939 b	8.8803	0.0804	0.0783	3.41	5348	0.94	0.81	[Fe/H]
HD 109271 b	7.8543	0.079	0.0786	-	5783	-	1.05	[Fe/H]
HD 158259 e	7.9510	-	0.0800	-	-	1.21	1.08	-
CoRoT-7 d	8.9660	-	0.0822	-	5250	-	0.92	-
TOI-837 b	8.3249	-	0.0835	8.631	6047	1.02	1.12	[Fe/H]
CoRoT-30 b	9.0601	0.0844	0.0845	11.31	5650	0.91	0.98	[Fe/H]
TOI-561 c	10.7788	0.0884	0.0891	2.91	5372	0.84	0.81	[Fe/H]
WASP-185 b	9.3876	0.0904	0.0905	14.011	5900	1.5	1.12	[Fe/H]
Kepler-427 b	10.2910	0.091	0.0914	13.79	5800	1.35	0.96	[Fe/H]
CoRoT-22 b	9.7560	0.092	0.0923	4.88	5939	1.14	1.1	[Fe/H]
HD 160691 d	9.6392	-	0.0924	-	5773	1.33	1.13	[Fe/H]

TOI-481 b	10.3311	0.097	0.0970	11.097	5735	1.66	1.14	[Fe/H]
HD 20003 b	11.8482	0.0974	0.0975	-	5494	-	0.88	[Fe/H]
TOI-763 c	12.2737	0.1011	0.1013	2.63	5450	0.9	0.92	[Fe/H]
WASP-130 b	11.5510	0.1012	0.1014	9.976	5625	0.96	1.04	[Fe/H]
Kepler-69 b	13.7223	0.094	0.1046	2.24	5638	0.93	0.81	[Fe/H]
HD 152843 b	11.6264	0.1053	0.1053	3.41	6310	1.43	1.15	[Fe/H]
HD 158259 f	12.0280	-	0.1055	-	-	1.21	1.08	-
TOI-2048 b	13.7902	-	0.1058	2.61	5185	0.79	0.83	[m/H]
HD 51608 b	14.0726	0.1059	0.1059	-	5358	-	0.8	[Fe/H]
TOI-1422 b	12.9972	0.108	0.1075	3.96	5840	1.02	0.98	[Fe/H]
HD 189567 b	14.2880	0.111	0.1083	-	5726	-	0.83	[Fe/H]
HD 45184 c	13.1354	0.11	0.1101	-	5869	-	1.03	[Fe/H]
HD 159243 b	12.6200	0.11	0.1102	-	6123	1.12	1.12	[Fe/H]
K2-37 d	14.0919	0.1103	0.1103	2.73	5413	0.85	0.9	[Fe/H]
HD 93385 c	13.1800	0.112	0.1107	-	5977	-	1.04	[Fe/H]
HD 1461 c	13.5052	0.1117	0.1118	-	5765	-	1.02	[Fe/H]
Kepler-67 b	15.7259	0.1171	0.1169	2.94	5331	0.78	0.86	[M/H]
HD 74698 b	15.0170	0.121	0.1207	-	5783	1.33	1.04	[Fe/H]
HD 20794 b	18.3150	0.1207	0.1208	-	5401	-	0.7	[Fe/H]
TIC 237913194 b	15.1689	0.1207	0.1212	12.52	5788	1.09	1.03	[Fe/H]
HD 179079 b	14.4790	0.1214	0.1215	-	5646	1.63	1.14	[Fe/H]
EPIC 249893012 c	15.6240	0.13	0.1244	3.67	5430	1.71	1.05	[Fe/H]
HD 31527 b	16.5535	0.1254	0.1255	-	5898	-	0.96	[Fe/H]
K2-292 b	16.9841	0.13	0.1294	2.63	5725	1.09	1	[Fe/H]
Kepler-129 b	15.7900	0.13	0.1302	2.4	5770	1.65	1.18	[Fe/H]
HATS-17 b	16.2546	0.1308	0.1309	8.709	5846	1.09	1.13	[Fe/H]
Kepler-66 b	17.8158	0.1352	0.1353	2.8	5962	0.97	1.04	[M/H]
HD 96700 c	19.8800	0.141	0.1382	-	5845	-	0.89	[Fe/H]
HD 21693 b	22.6786	0.1455	0.1456	-	5430	-	0.8	[Fe/H]
HD 167768 b	20.6532	0.1512	0.1512	-	4851	9.7	1.08	[Fe/H]
TOI-561 d	25.7124	0.158	0.1590	2.82	5372	0.84	0.81	[Fe/H]
TOI-1710 b	24.2834	0.16	0.1631	5.34	5665	0.97	0.98	[Fe/H]
HD 175607 b	29.0100	-	0.1649	-	5392	0.7	0.71	[Fe/H]
HD 28109 b	22.8910	0.1357	0.1705	2.199	6120	1.45	1.26	[Fe/H]
HD 191939 c	28.5797	0.1752	0.1706	3.195	5348	0.94	0.81	[Fe/H]
HD 152843 c	24.3800	-	0.1725	5.83	6310	1.43	1.15	[Fe/H]
HD 9446 b	30.0520	0.189	0.1893	-	5793	1	1	[Fe/H]
24 Boo b	30.3506	0.19	0.1899	-	4893	10.64	0.99	[Fe/H]
HD 224693 b	26.6904	0.191	0.1913	-	5894	1.93	1.31	[Fe/H]
HD 189567 c	33.6880	0.197	0.1919	-	5726	-	0.83	[Fe/H]
HD 109271 c	30.9300	0.196	0.1961	-	5783	-	1.05	[Fe/H]
HD 20003 c	33.9239	0.1964	0.1966	-	5494	-	0.88	[Fe/H]
HD 20794 c	40.1140	0.2036	0.2037	-	5401	-	0.7	[Fe/H]
HD 191939 d	38.3530	0.2132	0.2076	2.995	5348	0.94	0.81	[Fe/H]
EPIC 249893012 d	35.7470	0.22	0.2160	3.94	5430	1.71	1.05	[Fe/H]
61 Vir c	38.0210	0.2175	0.2169	-	5577	0.96	0.94	[Fe/H]
HD 45652 b	44.0730	0.237	0.2376	-	5294	0.94	0.92	[Fe/H]
HD 147018 b	44.2360	0.2388	0.2390	-	5441	-	0.93	[Fe/H]
HD 64114 b	45.7910	0.246	0.2464	-	5676	-	0.95	-
TOI-5678 b	47.7302	0.249	0.2497	4.91	5485	0.94	0.91	[Fe/H]
HD 93385 d	45.8500	0.2565	0.2541	-	5977	-	1.04	[Fe/H]
HD 21693 c	53.7357	0.2586	0.2588	-	5430	-	0.8	[Fe/H]
HD 31527 c	51.2053	0.2663	0.2663	-	5898	-	0.96	[Fe/H]
HD 34445 e	49.1750	0.2687	0.2688	-	5836	1.38	1.07	[Fe/H]
HD 28109 c	56.0082	0.308	0.3096	4.23	6120	1.45	1.26	[Fe/H]
NGTS-20 b	54.1892	0.313	0.3188	11.994	5980	1.78	1.47	[Fe/H]
TOI-561 e	77.0300	0.328	0.3304	2.55	5372	0.84	0.81	[Fe/H]
TOI-5542 b	75.1238	0.332	0.3353	11.31	5700	1.06	0.89	[Fe/H]
HD 20794 d	90.3090	0.3499	0.3499	-	5401	-	0.7	[Fe/H]
HD 21411 b	84.2880	0.362	0.3621	-	5605	-	0.89	-
HD 51608 c	95.9446	0.3809	0.3809	-	5358	-	0.8	[Fe/H]
HD 35759 b	82.4670	0.389	0.3886	-	6060	-	1.15	[Fe/H]
Kepler-129 c	82.2000	0.39	0.3912	2.52	5770	1.65	1.18	[Fe/H]

HD 191939 e	101.1200	0.407	0.3961	-	5348	0.94	0.81	[Fe/H]
HD 28109 d	84.2600	0.411	0.4065	3.25	6120	1.45	1.26	[Fe/H]
TOI-813 b	83.8911	0.423	0.4116	6.71	5907	1.94	1.32	[Fe/H]
HD 96700 d	103.5000	0.424	0.4152	-	5845	-	0.89	[Fe/H]
HD 206255 b	96.0450	0.461	0.4615	-	5635	-	1.42	-
61 Vir d	123.0100	0.476	0.4744	-	5577	0.96	0.94	[Fe/H]
HD 34445 d	117.8700	0.4817	0.4814	-	5836	1.38	1.07	[Fe/H]
Kepler-539 b	125.6324	0.4988	0.4992	8.373	5820	0.95	1.05	[Fe/H]
HD 20794 e	147.0200	0.509	0.5084	-	-	-	0.81	-
HD 37124 b	154.3780	0.53364	0.5337	-	-	-	0.85	[Fe/H]
HIP 14810 c	147.7470	0.549	0.5490	-	5544	1.07	1.01	[Fe/H]
HD 42618 b	149.6100	0.554	0.5536	-	5727	1	1.01	[Fe/H]
HIP 63242 b	124.6000	0.565	0.5641	-	4830	-	1.54	[Fe/H]
HD 9446 c	192.9000	0.654	0.6537	-	5793	1	1	[Fe/H]
Kepler-69 c	242.4613	0.64	0.7097	1.71	5638	0.93	0.81	[Fe/H]
HD 34445 c	214.6700	0.7181	0.7180	-	5836	1.38	1.07	[Fe/H]
HD 191939 g	284.0000	0.812	0.7886	-	5348	0.94	0.81	[Fe/H]
HD 159243 c	248.4000	0.8	0.8035	-	6123	1.12	1.12	[Fe/H]
HD 31527 d	271.6737	0.8098	0.8102	-	5898	-	0.96	[Fe/H]
TOI-2180 b	260.7900	0.828	0.8275	11.321	5695	1.64	1.11	[Fe/H]
HD 161178 b	279.3000	0.85	0.8530	-	4786	10.95	1.06	[Fe/H]
HD 124330 b	270.6600	0.86	0.8583	-	5873	-	1.15	[Fe/H]
HD 104985 b	199.5050	0.95	0.8824	-	4877	11	2.3	[Fe/H]
HD 79181 b	273.1000	0.9	0.8949	-	4862	11.06	1.28	[Fe/H]
HD 160691 e	307.9000	-	0.9299	-	5773	1.33	1.13	[Fe/H]
HD 219139 b	275.5000	0.94	0.9405	-	4831	11.22	1.46	[Fe/H]
HD 92788 b	325.8030	0.97	0.9713	-	5744	1.14	1.15	[Fe/H]
HD 360 b	273.1000	0.98	0.9817	-	4770	10.86	1.69	[Fe/H]
HD 155358 c	391.9000	1.02	1.0198	-	5900	-	0.92	[Fe/H]
Kepler-452 b	384.8430	1.046	1.0496	1.63	5757	1.11	1.04	[Fe/H]
TOI-1288 c	443.0000	-	1.0945	-	5225	1.01	0.89	[Fe/H]
HD 165155 b	434.5000	1.13	1.1307	-	5426	0.95	1.02	[Fe/H]
HIP 109384 b	499.4800	1.134	1.1346	-	5180	-	0.78	[Fe/H]
HD 173416 b	323.6000	1.16	1.1628	-	4683	13.5	2	[Fe/H]
ups Leo b	385.2000	1.18	1.1813	-	4836	11.22	1.48	[Fe/H]
HD 44219 b	472.3000	1.19	1.1875	-	5752	1.32	1	[Fe/H]
HD 75898 b	422.9000	1.191	1.1915	-	5963	1.58	1.26	[Fe/H]
HD 564 b	492.3000	1.2	1.2042	-	5902	1.01	0.96	[Fe/H]
HD 137496 c	479.9000	1.2163	1.2160	-	5799	1.59	1.04	[Fe/H]
HD 109286 b	520.1000	1.259	1.2578	-	5694	1.09	0.98	[Fe/H]
gam Psc b	555.1000	1.32	1.3180	-	4742	11.2	0.99	[Fe/H]
HD 17674 b	623.8000	1.42	1.4199	-	5904	1.18	0.98	[Fe/H]
Kepler-421 b	704.1984	1.219	1.4327	4.16	5308	0.76	0.79	[Fe/H]
BD-00 4475 b	723.2000	1.48	1.4705	-	5040	-	0.81	[Fe/H]
HD 210193 b	649.9180	1.487	1.4884	-	5790	-	1.04	-
HD 160691 b	645.0000	-	1.5224	-	5773	1.33	1.13	[Fe/H]
HD 34445 f	676.8000	1.543	1.5437	-	5836	1.38	1.07	[Fe/H]
HD 27969 b	654.5000	1.552	1.5508	-	5966	1.27	1.16	[Fe/H]
HD 64121 b	623.0000	1.51	1.6843	-	5078	5.44	1.64	[Fe/H]
HD 37124 c	885.5000	1.71	1.7103	-	-	-	0.85	[Fe/H]
HD 70573 b	851.8000	1.76	1.7594	-	5737	-	1	[Fe/H]
HD 147018 c	1008.0000	1.922	1.9213	-	5441	-	0.93	[Fe/H]
HIP 14810 d	981.8000	1.94	1.9406	-	5544	1.07	1.01	[Fe/H]
Kepler-539 c	1000.0000	2.42	1.9901	-	5820	0.95	1.05	[Fe/H]
Kepler-1654 b	1047.8356	2.026	2.0266	9.18	5597	1.18	1.01	[Fe/H]
HD 22532 b	872.6000	1.9	2.0780	-	5038	5.69	1.57	[Fe/H]
HD 68402 b	1103.0000	2.18	2.1707	-	5950	1.02	1.12	[Fe/H]
HD 9174 b	1179.0000	2.2	2.2068	-	5577	1.67	1.03	[Fe/H]
HD 29021 b	1362.3000	2.28	2.2793	-	5560	0.85	0.85	[Fe/H]
HD 221585 b	1173.0000	2.306	2.3077	-	5620	-	1.19	[Fe/H]
HD 134060 c	1291.5646	2.3928	2.3898	-	5966	-	1.09	[Fe/H]
81 Cet b	952.7000	2.5	2.5381	-	4785	11	2.4	[Fe/H]
HD 171238 b	1532.0000	2.57	2.5669	-	5440	1.01	0.96	[Fe/H]

HD 211810 b	1558.0000	2.656	2.6574	-	5652	1.13	1.03	[Fe/H]
HD 108874 c	1624.0000	2.659	2.6593	-	5551	-	0.95	[Fe/H]
HD 30669 b	1684.0000	2.69	2.6954	-	5400	0.91	0.92	[Fe/H]
HD 86226 b	1628.0000	2.73	2.7276	-	5863	1.05	1.02	[Fe/H]
HD 37124 d	1862.0000	2.807	2.8071	-	-	-	0.85	[Fe/H]
HD 167677 b	1820.0000	2.877	2.8792	-	5474	-	0.96	[Fe/H]
HD 129445 b	1840.0000	2.9	2.9302	-	-	-	0.99	[Fe/H]
HD 191939 f	2200.0000	3.2	3.0873	-	5348	0.94	0.81	[Fe/H]
HD 55696 b	1827.0000	3.18	3.1854	-	6012	1.52	1.29	[Fe/H]
HD 105779 b	2412.0000	3.38	3.3873	-	5792	0.94	0.89	[Fe/H]
HD 94771 b	2164.0000	3.48	3.4810	-	5631	1.9	1.2	[Fe/H]
HD 165131 b	2342.6000	3.54	3.5213	-	5870	-	1.06	[Fe/H]
Kepler-129 d	2646.0000	4	3.9581	-	5770	1.65	1.18	[Fe/H]
HD 74698 c	3449.0000	4.5	4.5284	-	5783	1.33	1.04	[Fe/H]
HD 115954 b	3700.0000	5	4.9496	-	5957	1.21	1.18	[Fe/H]
HD 160691 c	3947.0000	-	5.0934	-	5773	1.33	1.13	[Fe/H]
HD 154857 c	3452.0000	5.36	5.3583	-	5605	1.76	1.72	[Fe/H]
HD 134987 c	5000.0000	5.8	5.9099	-	5585	1.25	1.1	[Fe/H]
OGLE-2018-BLG	5480.0000	5	6.0859	-	5912	-	1	[Fe/H]
HD 34445 g	5700.0000	6.36	6.3902	-	5836	1.38	1.07	[Fe/H]
HD 150706 b	5894.0000	6.7	6.7319	-	5961	0.96	1.17	[Fe/H]
HD 50499 c	8619.9000	9.02	9.0067	-	6099	1.42	1.31	[Fe/H]
HD 92788 c	11611.2975	10.5	10.5186	-	5744	1.14	1.15	[Fe/H]
PZ Tel b	44000.0000	27	27.0366	-	-	-	1.36	-

## CONCLUSION

According to the correlation relationship between the mass and the radius of 2471 stars observe that the radius and mass of stars also share a strong positive correlation with value of 0.923792. This indicates that as stellar radius increases, stellar mass tends to increase as well. Similarly, as star radius decreases, star masses tend to decrease. In other words, an increase in mass is equivalent to an increase in radius and vice versa, that is, the relationship between mass and radius in stars is a direct relationship.  $M \propto R$ . Overall, these correlations suggest that there are relationships between the variables  $R$ ,  $M$ , and  $T$ . Changes in  $R$  and  $M$  tend to occur together, while changes in  $M$  and  $T$  also tend to occur together.

According to Fig 5, the correlation coefficient between mass and luminosity of 894 of 898 stars is 0.897892. This indicates a strong positive correlation between mass and luminosity. As mass increases, luminosity tends to increase as well. It's important to note that the Mass-Luminosity Relationship is an average relationship and there can be some variations among different stars due to other factors such as age, chemical composition, and stellar evolution.

For known values of luminosity of 3953 stars, only 933 stars luminosity was available (Fig 6). Accordingly, the correlation between luminosity and mass (L-M) found  $R^2 = 0.8966$  with the minimum and maximum mass of  $0.01 \leq M_s \leq 2.8$  in solar mass. The minimum and maximum luminosity is between -3.257 to 3.17 of solar luminosity. The size of selected stars is in the radius between 0.01 to 88.47 of solar radius with the mean value of 1.52213. The lowest and highest temperature observed among these stars is between 575 to 40000 kelvins. But here and after our calculation from total stars 3951 we found the unknown luminosities of 2918 stars. After computing star mass about  $0.01 \leq M_s \leq 2.8 M_\odot$  of solar

mass (same as Fig 6) the luminosity values of -3.252 to 3.192  $L_\odot$  in solar luminosity computed. The size of stars in terms of solar radius detected between 0.11 to 88.47  $R_\odot$  solar radius and the temperature between 2000 to 40000 Kelvins. The information shows a strong positive correlation between luminosity and star's mass in range of  $R^2 = 0.8803$ . This suggests that as stellar masses increase or decrease relative to solar masses, their computed luminosities also tend to increase or decrease proportionally (Fig 7). Also, a positive correlation between the luminosity and the radius of the stars about 0.505441 has been observed. This shows that as the calculated luminosities increase or decrease relative to the solar luminosities, the stellar radii tend to increase or decrease accordingly.

After computing of 2918 unknown luminosities, we observed 2121 stars are the in G-Type main sequence stars, between 5000 and 6000 Kelvin. The mass and luminosity stars are between  $0.47 \leq M_s \leq 1.96 M_\odot$  and  $-0.635 \leq L_s \leq 1.386 L_\odot$  in solar mass and luminosity respectively. The size of these stars is in the range of  $0.57 - 6.43 R_\odot$  of solar radius. The relationship between mass and luminosity of these type of stars (G-Type) display  $R^2 = 0.846$  that indicating a strong positive linear relationship between mass and luminosity. Additional stimulating results show correlations between temperature and luminosity (T-L) with  $R^2 = 0.6158$  and a luminosity and radius (L-R) of  $R^2 = 0.8297$ .

To investigating new exoplanets in the G-Type main sequence stars we observed a total of 248 exoplanets in the range of 5000 to 6000 Kelvin (Fig 9). In fact, this temperature range is of the G-Type stars. But in this region only 103 exoplanets had the physical conditions to study relationship between semi-major axis and orbital period.

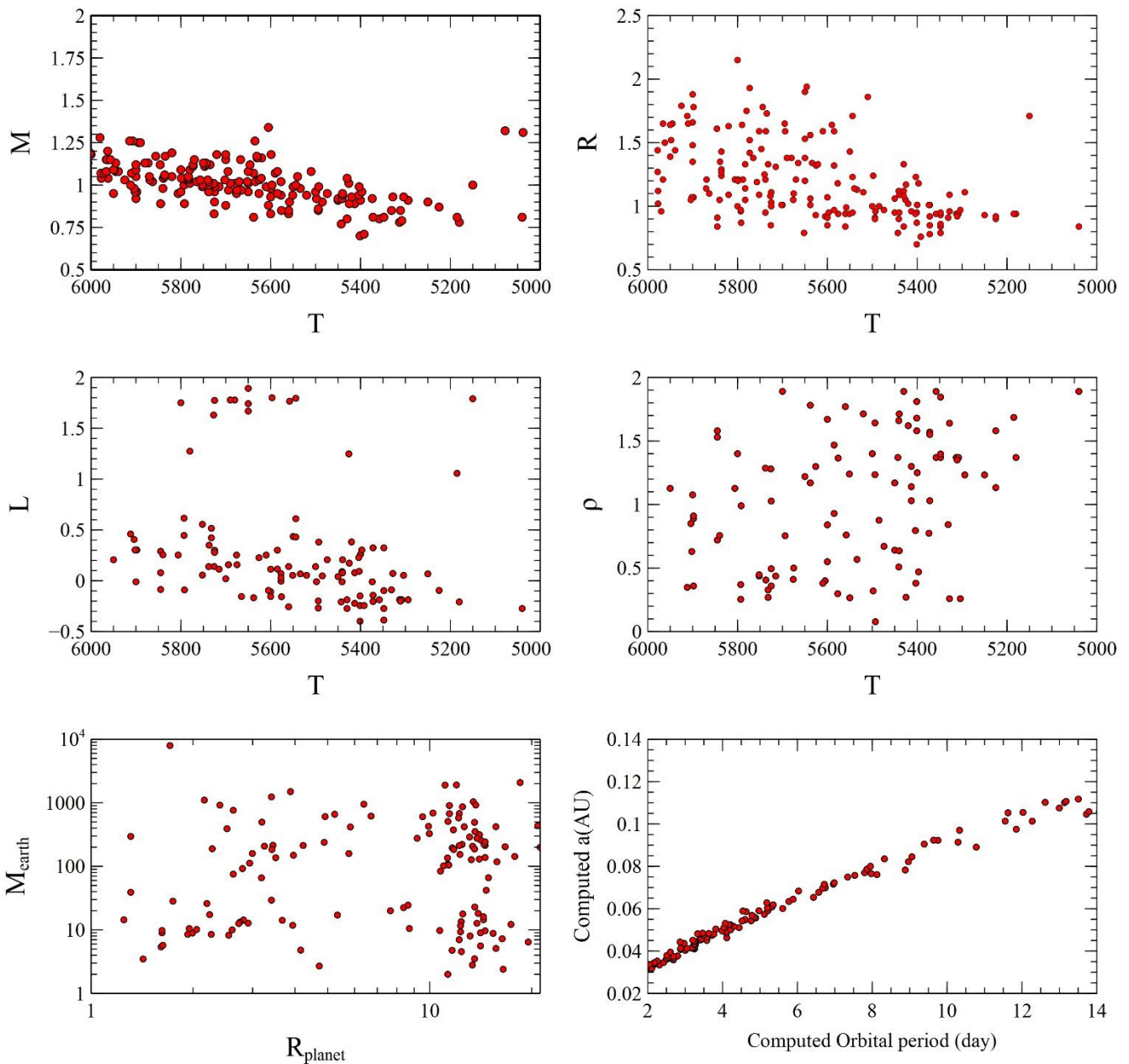


Fig 10: Relationship in G-Type main sequence stars and exoplanets

The results represents that the lower end of the range within which 5% of the data falls. The percentile values indicate that 5% of the planets have an orbital period of at least 1.1883 days, a semi-major axis of at least 0.0219425 AU, a size of at least 7.178, and an effective temperature of at least 5347 K. Similarly, about 10% of the planets have an orbital period of at least 1.57084 days, a semi-major axis of at least 0.02588 AU, a size of at least 9.134, and an effective temperature of at least 5402.7 K.

The values indicate that 25% of the planets have an orbital period of at least 2.41015 days, a semi-major axis of at least

0.0348825 AU, a size of at least 70.7158, and an effective temperature of at least 5543 K. Moreover, half of the planets have an orbital period of at least 3.46669 days, a semi-major axis of at least 0.04621 AU, a size of at least 207.543, and an effective temperature of at least 5685 K.

The correlation coefficient between the planet orbital period and the semi-major axis is about  $R^2 = 0.984969$ , which suggests a strong positive correlation. This means that as the orbital period increases, the semi-major axis of planets tends to increase as well.

## REFERENCES

- Abt, H. A., & Bidelman, W. P. J. A. J., vol. 158, p. (1969). Spectral classification of A-type spectroscopic binaries. 158, 1091.
- Bailer-Jones, C. A. J. a. p. a.-p. (2001). Automated stellar classification for large surveys: a review of methods and results.
- Brinchmann, J., Charlot, S., White, S. D., Tremonti, C., Kauffmann, G., Heckman, T., & Brinkmann, J. J. M. n. o. t. r. a. s. (2004). The physical properties of star-forming galaxies in the low-redshift Universe. 351(4), 1151-1179.
- Burnham, R. (2013). *Burnham's Celestial Handbook, Volume One: An Observer's Guide to the Universe Beyond the Solar System* (Vol. 1): Courier Corporation.
- Hernández, J. G., Delgado-Mena, E., Sousa, S., Israelian, G., Santos, N., Adibekyan, V. Z., . . . Astrophysics. (2013). Searching for the signatures of terrestrial planets in F-, G-type main-sequence stars. 552, A6.
- Hertzsprung, E. (1947). Catalogue de 3259 étoiles dans les Pléiades. *Annalen van de Sterrewacht te Leiden*, vol. 19, pp. A1-A89, 19, A1-A89.
- Inglis, M. (2015). The Hertzsprung-Russell Diagram. In *Astrophysics Is Easy!* (pp. 77-84): Springer.
- Institute, N. E. S. (2020). Planetary Systems Table. In: IPA.
- Jaschek, C., & Jaschek, M. (1990). *The classification of stars*: Cambridge university press.
- Morgan, W. W., Keenan, P. C., & Kellman, E. (1943). An atlas of stellar spectra. In: Chicago: University of Chicago Press.
- Morgan, W. W., Keenan, P. J. A. R. o. A., & Astrophysics. (1973). Spectral classification. 11(1), 29-50.
- Percy, J. R. (2007). *Understanding variable stars*: Cambridge University Press.
- Pickering, E. C. J. A. o. H. C. O., vol. 27, pp. 1-388. (1890). The Draper Catalogue of stellar spectra photographed with the 8-inch Bache telescope as a part of the Henry Draper memorial. 27, 1-388.
- Wilson, M. W., Childs, K. P., & Edith, K. (1943). An atlas of stellar spectra, with an outline of spectral classification.